JOURNAL OF NANOMATERIALS AND APPLICATIONS

Journal of Nanomaterials and Applications

Journal homepage: https://jna.com.vn

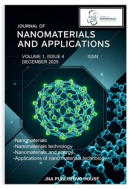

Structure–Property Relationships and Multi-Objective Design in Advanced Metallic Systems: From Nanocrystals and High-Entropy Alloys to Bulk Metallic Glasses

Burak Malik Kaya [1,*], Selcuk Temiz [2], Umut Sarac [3]

[1] Eskisehir Osmangazi University, Vocational School of Health Service, 26480, Eskisehir, Turkey
[2] Department of Physics, Eskisehir Osmangazi University, Eskisehir 26040, Turkey
[3] Bartın University, Department of Science Education, 74100, Bartın, Turkey

Review info
Type of articles:
Review article

Corresponding author*:
Burak Malik Kaya:
vidyasingh005@gmail.com

Received: 06 July 2026
Revised: 09 August 2026
Accepted: 12 August 2026
Published: 28 August 2026

Abstract: This review provides a comprehensive analysis of nanostructured metals, high-entropy alloys (HEAs), and bulk metallic glasses (BMGs), focusing on structure–property relationships across atomic, defect, and microstructural scales. This review elucidates the fundamental processing routes and governing mechanisms responsible for structural evolution across nanostructured metallic systems. Furthermore, recent evidence re-evaluating sluggish diffusion in HEAs and mechanisms ensuring structural stabilization are critically examined. Differences in atomic diffusion kinetics across the three material classes are systematically delineated. Finally, an AI-assisted framework and multi-objective design roadmap are presented for future intelligent metallic systems in aerospace, green energy, and biomedical applications.

Keywords: Nanostructured metals; High-entropy alloys; Grain boundary engineering; Strength-ductility trade-off; Passivation & Corrosion resistance

1. Introduction

In the era of Industry 4.0 and the pursuit of Net-Zero, traditional metallic materials are facing serious physical limitations. Simultaneously optimizing strength and ductility, or enhancing electrical conductivity without compromising heat resistance, has been been a challenging problem for decades. The advent of nanostructuring and the design philosophy of high-entropy alloys (HEAs) has significantly advanced in materials science. By precisely controlling structures from the atomic level and grain boundaries to nano-precipitation phases, scientists have redefined the performance limits of metals, transforming them into "smart materials" capable of withstanding the harshest environments [1, 2]. In

the last decade, advances in electrochemical deposition techniques have further enabled the synthesis of high-quality nanostructured thin films with tailored microstructures, surface morphologies, and functional properties. Studies on ternary alloy thin films have demonstrated the strong influence of deposition parameters – such as bath temperature, applied current density, and potential – on magnetic features, coercive force, and surface texture [3–6]. These findings highlight the versatility of electrochemical methods for producing multifunctional metallic coatings. The shift in the global technology map does not diminish the role of metallic materials; on the contrary, it demands a revolutionary evolution. Metallic materials have evolved from conventional structural components to multifunctional engineering platforms capable of simultaneously delivering mechanical integrity and functional performance [7]. Studies on Schottky barrier diodes and heterojunction structures have further demonstrated the critical importance of interface engineering for achieving tunable electrical properties, such as barrier heights and temperature-dependent current-voltage characteristics [8,9]. In future infrastructure systems, the dual integration of ultra-high mechanical properties and tunable physical properties (magnetism, electrical properties, chemical corrosion resistance) allows significant reductions in structural weight, optimization of energy efficiency, and extension of operational life significantly. Rather than simply using a single base metal (such as traditional iron, aluminum, titanium), the multi-element systems assembled and modified at the nanoscale is a progress for addressing the technical barriers of the 21st century [7]. The ability to precisely manipulate and control lattice defects and phase boundaries at the nanoscale opens up unprecedented application corridors in three strategic industrial pillars:

Aerospace and Advanced Defense: Heat-resistant nanoalloys and refractive HEAs are capable of maintaining superior tensile strength limits at temperatures exceeding conventional thresholds [10]. This capability is critical for manufacturing high-efficiency jet engine turbine blades, hypersonic-resistant ultralight spacecraft hulls, and high-speed impact systems without creep or material fatigue. Furthermore, the exceptional thermal stability and oxidation resistance of these materials enable prolonged operation under extreme thermomechanical loads, significantly improving engine thrust-to-weight ratios and vehicle survivability in hypersonic flight regimes. By leveraging heterogeneous microstructures and coherent nanoprecipitates, these advanced alloys also offer enhanced damage tolerance against thermal shocks and cyclic fatigue, paving the way for next-generation propulsion systems and re-entry vehicles that outperform today's state-of-the-art nickel-based superalloys [11].

Green energy infrastructure and digital transformation: The combination of nano-twin structures and hierarchical carbon networks (graphene/CNTs) creates next-generation conductors that break Nordheim's law, achieving ultra-high maximum current density [12]. This application directly solves the energy consumption problem in smart grids and supercomputers. At the same time, nanoporous metals with exceptionally high specific surface area act as ideal electrochemical catalytic membranes for the clean hydrogen energy supply chain, serving well for fuel cells and electrochemical water splitting [13]. Their three-dimensional interconnected porous networks facilitate rapid mass transport and maximize active site exposure, delivering superior bifunctional performance in hydrogen evolution reaction (HER) and oxygen evolution reaction (OER) with enhanced durability compared to conventional catalysts.

Smart biomedical and minimally invasive: Highly biocompatible amorphous alloys and nanostructured metals can accurately mimic the elastic modulus of human bone, eliminating stress

shielding that causes bone resorption in artificial joints [14]. In particular, the trend of developing biodegradable metals at the nanoscale allows implantable devices such as vascular stents or bone plates to safely decompose in the body after completing their medical function, completely eliminating the need for a second surgery to remove the device [15]. Furthermore, these materials enable controlled degradation profiles that can be tailored to match the rate of tissue regeneration, providing temporary structural support while gradually transferring load to the healing bone or vascular tissue. This dynamic biocompatibility represents a significant leap toward patient-specific, regenerative implant technologies. Although numerous review articles [16-18] have summarized individual classes of advanced metallic materials, a comprehensive framework integrating nanostructure engineering, multifunctional properties, artificial intelligence-assisted alloy design, and industrial deployment remains largely unavailable. To address this gap, this review explicitly highlights three unique contributions compared to existing literature: (1) establishing a cross-material unified structure–property–performance map spanning nanostructured metals, HEAs, and BMGs; (2) elucidating the physical mechanisms that simultaneously overcome multi-property trade-offs (e.g., strength–ductility, strength–conductivity, and strength–corrosion kinetics); and (3) mapping the integration of machine learning surrogate modeling with autonomous self-driving laboratories for rapid materials discovery. The structural evolution of these advanced systems is governed by distinct thermodynamic and kinetic driving factors: (i) in nanocrystalline metals, severe plastic deformation (SPD) strain amplitude, stacking fault energy (SFE), and grain boundary segregation drive grain refinement and boundary complexion transitions; (ii) in HEAs, configurational entropy, lattice strain mismatch (δ), and chemical short-range order (CSRO) dictate phase stability; and (iii) in BMGs, critical cooling rates, atomic radius mismatch, and free-volume distribution govern the retention of topological amorphous states.

1.1. Methodology of Literature Review

This review was conducted using a systematic literature survey approach following the Preferred Reporting Items for Systematic Reviews and Meta-Analyses (PRISMA) framework. Scientific publications were collected from Web of Science, Scopus, and ScienceDirect databases covering the period from January 2000 to March 2026. The search strategy employed combinations of the keywords “nanostructured metals”, “grain boundary engineering”, “high-entropy alloys”, “bulk metallic glasses”, “nanotwinned metals”, “corrosion resistance”, “mechanical properties”, and “machine learning for materials design”. Initially, 512 publications in total were qualified. After removing duplicate records and excluding conference abstracts, non-English publications, and articles lacking sufficient experimental validation, 146 peer-reviewed papers were selected for detailed analysis. The selected literature was classified into four categories:

i) Structural engineering and microstructural control.

ii) Mechanical strengthening mechanisms.

iii) Functional properties.

iv) Future intelligent metallic systems.

This systematic classification enables the establishment of quantitative relationships between microstructure evolution and material performance while identifying critical challenges for industrial deployment [19-22]. Despite remarkable advances in nanostructured metallic systems, most existing studies focus on isolated performance metrics such as strength, corrosion resistance, or magnetic behavior. Comprehensive understanding of the coupling effects among multiple functional properties

remains limited. Furthermore, scalability, thermal stability, and lifecycle sustainability continue to hinder the transition of advanced metallic materials from laboratory-scale demonstrations to industrial deployment. Current literature also lacks unified frameworks linking nanostructure design, deformation mechanisms, and data-driven materials discovery. The present review addresses these gaps by integrating structural engineering, functional performance, and artificial intelligence-assisted alloy design into a single analytical framework [23–25].

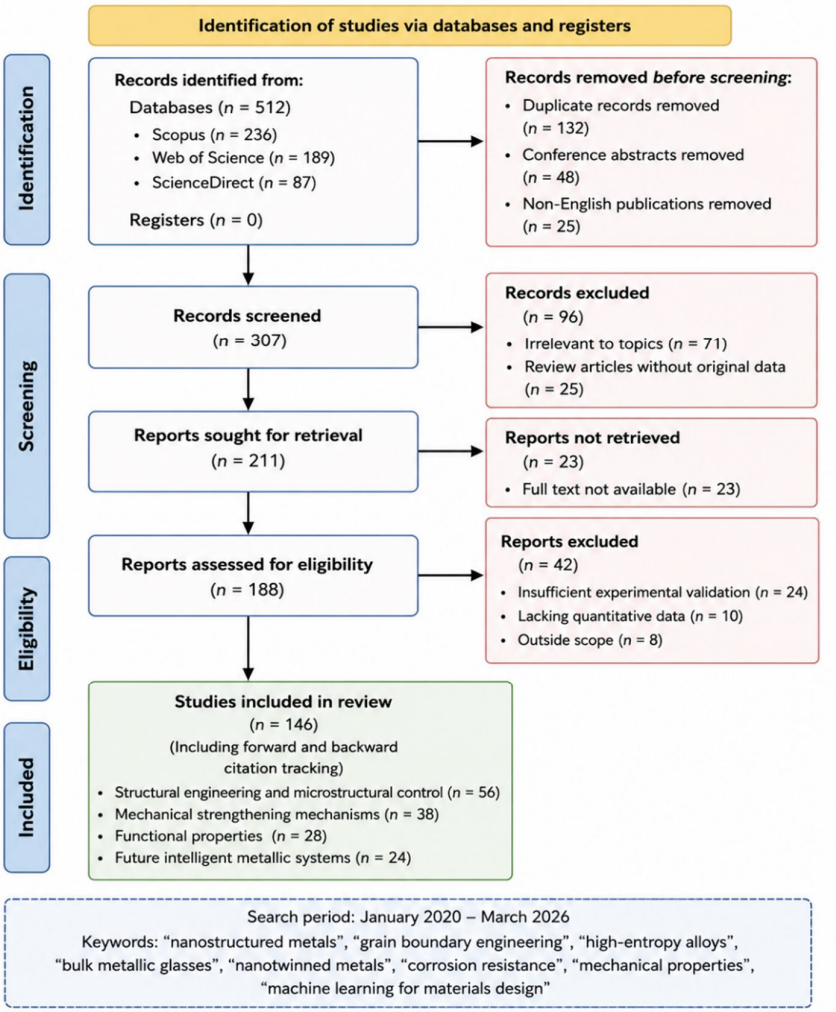

Figure 1. PRISMA flow diagram demonstrating literature screening and selection process.

2. Advances in Structural Characterization

Advanced Structural Characterization of materials severe plastic deformation (SPD) techniques such as equal-channel angular pressing (ECAP) and high-pressure torsion (HPT), reveals that these methods do more than simply referring grain size below 100 nm. They primarily generate extremely high dislocation densities, often exceeding 10^{16} m^{-2}, which serve as the driving force for dynamic recrystallization and the formation of stable ultrafine-grained or nanocrystalline structures [26, 27].

2.1. Particle Boundary and Nanophase Control

The period 2020–2026 witnessed the explosion of Advanced Structural Characterization techniques such as ECAP or HPT, allowing for uniform reduction of particle size to below 100 nm [28]. A recent research highlight is the concept of "Grain Boundary Engineering" (GBE), which focuses on the intentional

manipulation of grain boundary character distribution to enhance mechanical properties, corrosion resistance, and thermal stability of ultrafine-grained materials [29, 30]. Instead of vulnerable random grain boundaries, researchers focus on creating nanotwinned GBEs and fractional low-energy grain boundaries [31]. The appearance of self-healing nano-precipitates at the grain boundaries acts as a "pinning effect," preventing grain growth at high temperatures, significantly mitigating the weakness of poor thermal stability of traditional nanomaterials [32]. The kinetics of this particle boundary locking process are strongly reinforced by phase-field simulations and high-resolution transmission electron microscopy (HR-TEM). As the nanostructured precipitated phases are densely distributed along the particle boundaries, they generate Zener pinning forces (FZ) that hinder particle boundary movement, which are determined through theoretical stereochemical interaction models [31-33]:

$$F_Z = \frac{3\gamma_{GB} f}{2r} \quad (1)$$

In Eq. 1, f represents the surface free energy of the grain boundary, f is the volume fraction of the nano-precipitated phases and r is the average radius of the precipitated particle. Thermodynamic equilibrium at this interface suppresses the dynamics of grain growth, completely resolving the weakness of thermal stability of traditional nanomaterials when operating under high temperature or prolonged mechanical stress conditions [28, 33].

2.2. High Entropy Alloys (HEAs) and Amorphous Metals (BMGs)

Unlike conventional alloys that are commonly based on one or two principal elements, high-entropy alloys (HEAs) consist of five or more principal elements in near-equiatomic proportions. This multi-principal element approach leads to a significantly high configurational entropy, which stabilizes simple solid-solution phases (such as FCC, BCC, or HCP) and suppresses the formation of complex intermetallic compounds – a phenomenon known as the high-entropy effect [34]. This unique thermodynamic stabilization enables HEAs to exhibit exceptional combinations of strength, thermal stability, ductility, and corrosion resistance, often surpassing traditional alloys in extreme environments [35].

Core Effects of HEA:

The core effects in HEAs include severe lattice distortion, sluggish diffusion that suppresses coarse phase separation, and the so-called “cocktail” effect, which enables synergistic optimization of overall properties through complex elemental interactions [35]. In parallel, bulk metallic glasses (BMGs) with short-range order and grain boundaryless structure continue to improve ductility by implanting nanocrystalline composites, minimizing the formation of catastrophic shear bands [36]. These distinct strengthening and toughening mechanisms are clearly reflected in the mechanical performance of representative advanced metallic systems (Table 1). For instance, while nanocrystalline copper achieves high yield strength through grain refinement, CoCrFeMnNi HEAs and Ti-based BMGs offer superior combinations of strength and ductility or corrosion resistance, demonstrating the advantages of different microstructural design strategies. The recent development of advanced metallic materials has highlighted the necessity of establishing quantitative relationships between microstructural features and engineering performance. For nanostructured metals, grain refinement significantly increases yield strength through Hall–Petch strengthening. Experimental investigations reveal that reducing grain size from 10 μm to 100 nm may increase yield strength by nearly an order of magnitude [37]. In HEAs, severe lattice distortion contributes to enhanced solid-solution strengthening. The resulting resistance to dislocation motion generates superior strength while maintaining acceptable ductility [38]. For metallic glasses, the absence

of grain boundaries eliminates conventional weak points for corrosion and crack initiation. However, the formation of localized shear bands remains a major challenge limiting plastic deformation [39]. These observations indicate that future material design should prioritize synergistic optimization rather than maximizing a single property.

Table 1. Comparison of representative advanced metallic systems [37-39]

Material	Yield Strength (MPa)	Elongation (%)	Corrosion Resistance
Nanocrystalline Cu	800–1200	5–10	Moderate
CoCrFeMnNi HEA	700–1000	40–60	Excellent
Ti-based BMG	1500–2200	2–5	Excellent
Refractory HEA	1200–1800	10–20	Very High

2.3 Comparative Structure–Property Relationships

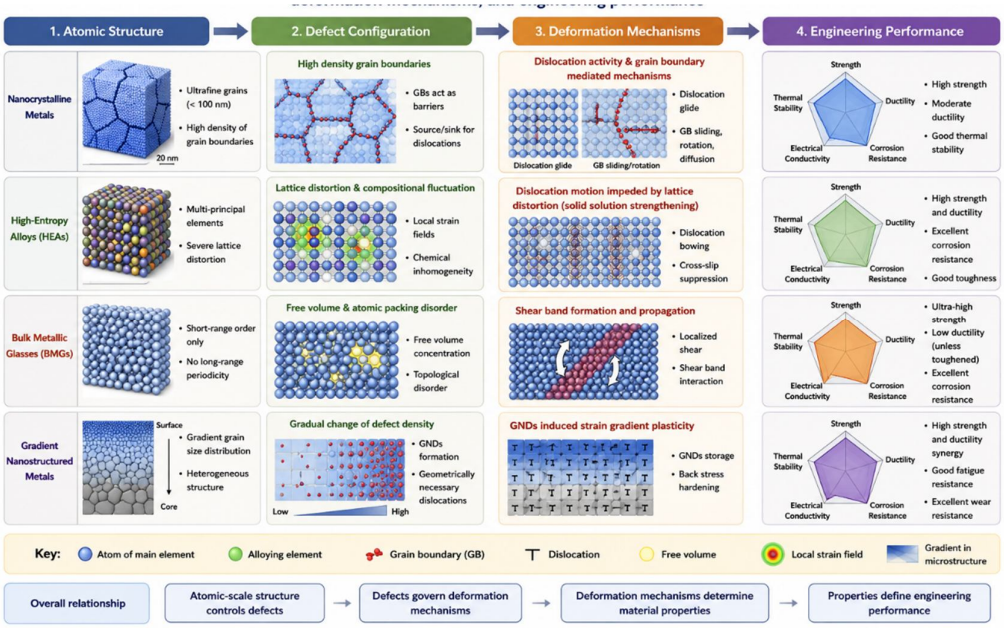

Figure 2 summarizes the hierarchical relationships between atomic structure, defect Although nanocrystalline metals, HEAs, and bulk metallic glasses (BMGs) all belong to the family of advanced metallic materials, their exceptional performances originate from fundamentally different structural characteristics. Understanding these distinctions is essential for establishing rational materials design strategies.

Figure 2 provides a comprehensive hierarchical framework that summarizes the structure–property relationships across advanced metallic materials. It illustrates how atomic structure and defect configuration govern deformation mechanisms, which in turn determine engineering performance in nanocrystalline metals, high-entropy alloys (HEAs), and bulk metallic glasses (BMGs). This integrated perspective highlights the distinct strengthening strategies and limitations of each material class configuration, deformation mechanisms, and engineering performance.

As shown in Table 2, nanocrystalline metals primarily rely on Hall–Petch strengthening but face thermal instability, whereas HEAs benefit from severe lattice distortion and solid-solution strengthening at the expense of higher alloy cost. Gradient nanostructured metals leverage GND (geometrically necessary dislocation) strengthening, and BMGs derive their strength from dense atomic packing, albeit limited by shear band localization. These comparative insights underscore the importance of adopting a systems-level approach in future materials design, where microstructural features are deliberately engineered to overcome individual limitations through synergistic optimization.

Table 2. Comparative structure–property relationships of representative advanced metallic systems

Material	Dominant structural feature	Primary strengthening mechanism	Major limitation	Future strategy
Nanocrystalline metals	High grain boundary density	Hall–Petch + nanotwins	Thermal instability	Grain boundary engineering
Gradient nanostructured metals	Gradient grain size	GND strengthening	Complex fabrication	Additive manufacturing
HEAs	Severe lattice distortion	Solid solution strengthening	High alloy cost	AI-assisted composition optimization
BMGs	Amorphous structure	Atomic packing	Shear localization	Nanocrystal toughening

2.3.1 Grain-boundary dominated nanostructured metals

Nanocrystalline metals derive their superior strength primarily from extremely high density of grain boundaries. Grain refinement enhances dislocation storage capacity while suppressing dislocation pile-up, producing Hall–Petch strengthening over a wide range of grain sizes. However, as grain size decreases to the nanoscale – particularly approaching approximately 10 nm – a fundamental transition occurs from conventional dislocation-mediated plasticity to grain-boundary-mediated deformation mechanisms [37]. At this critical scale, the classical Hall–Petch relationship breaks down, and in some cases, an inverse Hall–Petch softening effect is observed when grain boundary sliding and diffusion become dominant [40]. To mitigate this transition and maintain high strength at the nanoscale, recent strategies such as grain-boundary complexion engineering, the introduction of nanotwins, and nanoprecipitate pinning have proven highly effective. These approaches stabilize grain boundaries against migration and sliding, thereby delaying the onset of softening and extending the beneficial regime of Hall–Petch strengthening [41].

2.3.2 Lattice-distortion controlled HEAs

Unlike conventional alloys that rely primarily on one or two principal elements, HEAs drive their mechanical strengthening from severe lattice distortion caused by the incorporation of multiple principal elements in near-equiatomic proportions [42]. The random occupation of lattice sites by atoms with different atomic radii generates significant local elastic strain fields, which act as potent obstacles to dislocation motion. Simultaneously, compositional fluctuations at the atomic scale increase the lattice friction stress while preserving relatively high work-hardening capacity through dynamic interactions between dislocations and the heterogeneous atomic environment [43]. Recent atomistic simulations and density functional theory calculations further reveal that lattice distortion not only modifies the local electronic density of states but also collectively influences diffusion kinetics, stacking fault energy, and phase stability [44].

Consequently, HEAs frequently exhibit a remarkable synergy of mechanical and functional properties rarely achieved in conventional alloys. These include high yield strength, excellent ductility, remarkable fracture toughness, and outstanding corrosion resistance. This unique combination arises from the coupled effects of severe lattice distortion, sluggish diffusion, and the so-called “cocktail” effect, making HEAs particularly attractive for structural applications under extreme conditions.

2.3.3 Topological disorder in metallic glasses

BMGs differ fundamentally from crystalline alloys because they possess only short-range atomic order without periodic lattice structures [39]. The absence of conventional grain boundaries eliminates preferred sites for corrosion initiation and significantly reduces micro-galvanic coupling, thereby imparting excellent corrosion resistance. Nevertheless, plastic deformation in monolithic BMGs is highly localized through the formation of shear bands, which often leads to catastrophic failure with limited macroscopic ductility.

Recent investigations have demonstrated that the strategic introduction of nanocrystals or dual-phase heterostructures within the amorphous matrix effectively redistributes local stress concentrations and promotes the formation of multiple, mutually interacting shear bands rather than a single dominant catastrophic shear band [45]. This structural heterogeneity activates additional plastic deformation mechanisms, such as shear-band branching, deflection, and multiplication, resulting in a substantial enhancement of tensile ductility while maintaining an ultra-high yield strength that frequently exceeds 2 GPa in optimized systems [46]. Such improvements arise from the synergistic interaction between the amorphous matrix and the embedded crystalline phases, which hinder shear-band propagation and enable more homogeneous plastic flow. These findings highlight the potential of topological disorder engineering as a powerful strategy to overcome the intrinsic brittleness of metallic glasses, paving the way for their broader application in structural components requiring both high strength and adequate toughness.

2.3.4 Comparative deformation mechanisms

The dominant strengthening and deformation mechanisms vary substantially across nanocrystalline (NC) metals, high-entropy alloys (HEAs), and bulk metallic glasses (BMGs), leading to distinct mechanical responses even at comparable yield strengths [47,48]. In nanocrystalline metals, grain refinement to the nanoscale primarily activates Hall–Petch strengthening through dislocation pile-ups at grain boundaries, supplemented by dislocation accumulation, nanotwin formation, and grain-boundary pinning or sliding. At very small grain sizes (typically below ~10–20 nm), a transition occurs toward grain-boundary-mediated processes, including sliding, rotation, and partial dislocation emission, which can result in an inverse Hall–Petch effect and modified ductility [49,50]. HEAs, by contrast, derive their strength primarily from solid-solution strengthening intensified by severe lattice distortion due to atomic size mismatches among multiple principal elements. Additional contributions come from sluggish diffusion (which hinders defect mobility) and deformation-induced mechanisms such as transformation-induced plasticity (TRIP) and twinning-induced plasticity (TWIP). These enable dynamic Hall–Petch-like effects via twin or phase boundaries that refine the effective microstructure during straining, often promoting superior strength-ductility synergies [51,52]. In BMGs, plastic deformation is governed by the amorphous structure and relies on atomic packing density, free-volume creation and redistribution, shear transformation zones (STZs), and the nucleation, propagation, and interaction of shear bands. Nanocrystal-assisted strain redistribution or shear-band multiplication can enhance ductility in select cases, but localization into dominant shear bands often limits macroscopic plasticity [48,53]. These fundamentally different pathways—dislocation/grain-boundary dominated in NC metals, lattice-distortion and metastability-driven in HEAs, and shear-band/free-volume mediated in BMGs—explain why materials with similar yield strengths can exhibit markedly different ductility, work hardening, and failure behaviors.

2.3.5 Multi-objective property optimization

A prominent trend in alloy development since the early 2010s, accelerating markedly in the past five to ten years, is the shift from single-property maximization toward simultaneous optimization of multiple, often competing functional attributes [54]. Instead of pursuing peak strength alone, contemporary efforts target balanced performance envelopes encompassing strength, ductility, fatigue resistance, corrosion resistance, electrical/thermal conductivity, microstructural stability, and manufacturability. Machine-learning (ML) frameworks, particularly Bayesian optimization (BO) variants (including multi-objective, hierarchical deep Gaussian process, and batch BO), along with graph neural networks and generative models, have dramatically accelerated this transition. These approaches enable efficient navigation of vast compositional spaces, identifying Pareto-optimal solutions with far fewer experiments than traditional trial-and-error methods [55-57]. Recent studies on HEAs demonstrate successful application to coupled mechanical-magnetic, strength-ductility, or thermomechanical objectives, often integrating physics-informed surrogates and active learning [55, 58].

2.3.6 Unified structure–property map

Overall, the comparative analysis demonstrates that advanced metallic systems no longer follow a single strengthening philosophy.

Instead,

Atomic configuration

↓

Defect engineering

↓

Microstructural hierarchy

↓

Deformation mechanism

↓

Functional properties

↓

Engineering performance

forms a unified multiscale design pathway.

Future alloy development will increasingly combine nanoscale structural engineering, artificial intelligence, and autonomous experimentation to optimize multiple performance objectives simultaneously rather than maximizing only one individual property [59-65].

2.3.7 Distinguishing Diffusion Mechanisms Across Advanced Metallic Architectures: Fundamental differences exist in the atomic transport kinetics among the three material classes:

Nanocrystalline Metals: Diffusion is dominated by short-circuit grain boundary pathways (D_{GB} \ D_v). Radiotracer profiling (Harrison B/C regimes) and Atom Probe Tomography (APT) demonstrate that grain boundary diffusion rates are several orders of magnitude faster than lattice diffusion, accelerating surface oxidation and low-temperature phase transformations.

High-Entropy Alloys (HEAs): Atomic migration involves multi-component interdiffusion governed by localized lattice distortion and variable vacancy formation energies. Tracer diffusion studies (D^*) using diffusion couples show that diffusion kinetics are strongly dependent on local atomic configurations and element-specific activation energy barriers rather than uniform sluggishness.

Bulk Metallic Glasses (BMGs) & Bulk Crystals: While conventional bulk crystals rely strictly on vacancy-mediated lattice hopping, amorphous BMGs exhibit cooperative, multi-atomic movement enabled by localized free-volume fluctuations. Quasi-Elastic Neutron Scattering (QENS) confirms that atomic movement in BMGs undergoes structural relaxation below glass transition temperatures (T_g) without crystalline lattice constraints.

3. Magnetic Properties at the Nanoscale

When the size of metal particles decreases below the magnetic domain wall width (usually from 10 - 50 nm), the material transitions from a multi-domain to a single-domain magnetic state, leading to Superparamagnetism [66].

3.1. Optimization of coercivity (Hc) and saturation magnetization (Ms)

Research from 2022 to the present has focused on transition metal nanoparticles (Fe, Co, Ni) encased in carbon nanoshells or oxides (core-shell structures) to protect the core from oxidation while maintaining extremely high M_s [67]. For rare earth-free permanent magnets, the exchange-spring mechanism nanostructure between the hard magnetic nanophase (such as L10-FePt) and the soft magnetic nanophase (α-Fe) has achieved superior maximum magnetic energy product BHmax due to quantum exchange coupling at the nano interface [68]. The essence of this superiority lies in the optimization of the quantum interaction distance at the phase boundary. For the exchange coupling phenomenon to occur optimized without being degraded by local magnetic inversion, the size of the soft magnetic phase (α-Fe) must be less than twice the thickness of the magnetic domain wall of the hard magnetic phase [66]. Micromagnetic simulations show that the interlocking atomic-scale distribution of these phases allows the magnetic anisotropy energy of the hard phase to be efficiently transferred to the soft phase, enabling the magnet to have both exceptionally high coercivity (H_c) and maintain saturation magnetization (Ms) close to the theoretical level [67, 68].

3.2. Future Magnetic Applications

Ultra-high density data storage: Using new generation multilayer metal nano-magnet-resistance (GMR) and tunnel resistance (TMR) thin films. Biomedical: Fe-Cr-Ni biocompatible magnetic nanoparticles are used in hyperthermia to kill cancer cells and as high-current contrast agents in MRI imaging [69].

4. Extraordinary Mechanical Properties

4.1. Mechanisms for stabilizing nanostructures

According to the Hall-Petch law, the yield limit (σ_y) increases as the particle size (d) decreases:

$$\sigma_y = \sigma_0 + k_y d^{-1/2} \quad (2)$$

A quantitative assessment of Hall–Petch strengthening demonstrates the substantial influence of grain refinement on mechanical performance. For pure copper, the yield strength increases from approximately 70 MPa at grain sizes above 50 μm to more than 1.2 GPa when grain size approaches 20 nm [71]. However, experimental observations indicate that further grain refinement below approximately 10 nm triggers the inverse Hall–Petch phenomenon due to grain boundary-mediated deformation mechanisms replacing conventional dislocation motion [72]. However, when d < 10nm, the Hall-Petch law is reversed (Inverse Hall-Petch) due to the particle boundary slip mechanism replacing the dislocation movement [73].

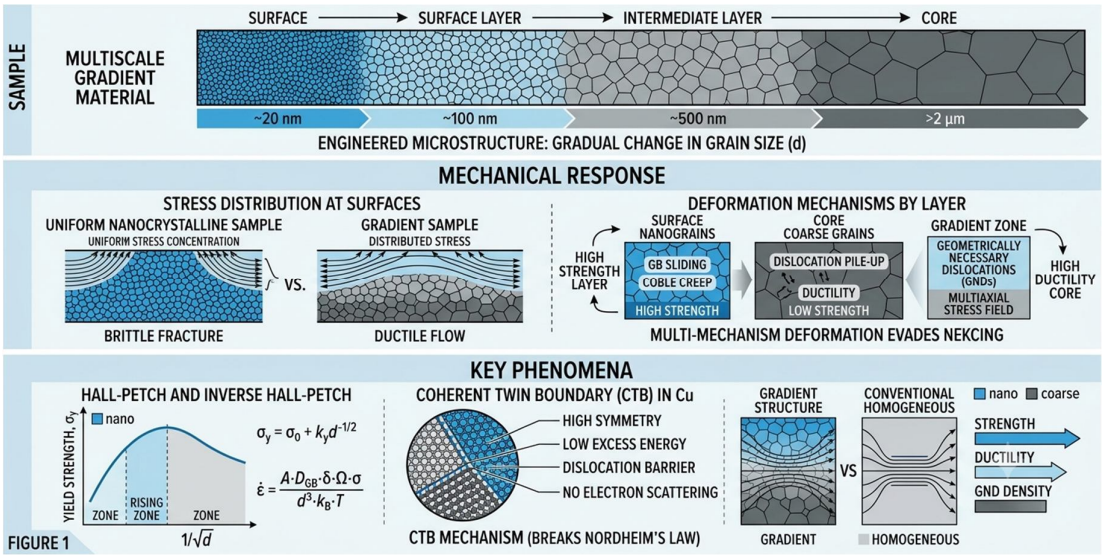

Figure 3 New Hall–Petch vs Inverse Hall–Petch Source: Koch (2024) [70]

When the grain boundaries approach the size of the super-nano structure (d < 10 nm), the space within the grain is no longer sufficient for dislocations to reproduce or move.

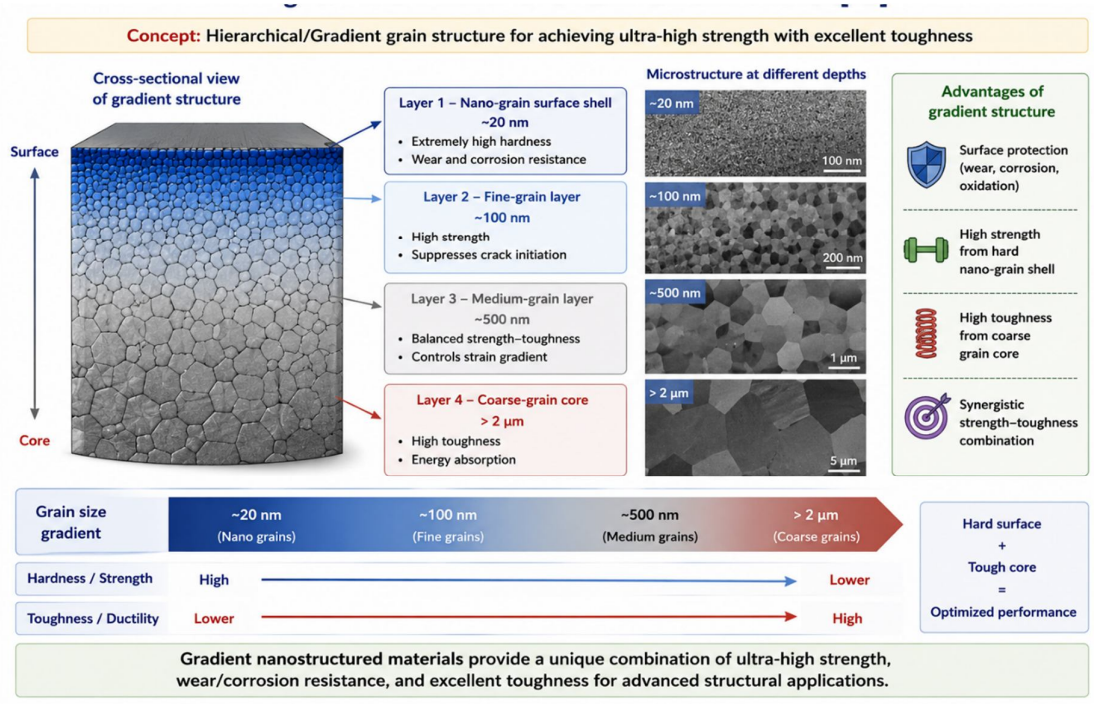

Figure 4 New Gradient Nanostructured Materials [74]

At this point, the grain boundary creep mechanism becomes dominant and the plastic strain rate (ε) of the material is quantified through the diffusion kinetic equation [73, 74]:

$$\varepsilon = \frac{AD_{GB}\delta\Omega\sigma}{d^3 k_B T} \quad (3)$$

Where: D_{GB} is the particle boundary diffusion coefficient, δ is the effective width of the particle boundary, Ω is the atomic volume, and ε is the applied mechanical stress. To overcome the softening phenomenon caused by the inverted Hall-Petch, the Gradient Nanostructured Materials architecture has been developed [74]. By designing a continuous change in particle size from the surface shell (superhard

nanoparticles) to the center of the material (tough microparticles), the material generates the necessary geometric dislocations (GNDs), creating a multi-axis stress field that evenly distributes the tensile load, resulting in a dual combination of ultra-high strength and excellent toughness [75].

To achieve ultra-high strength without brittleness, Hierarchical/Gradient grain structures have been developed: the material core consists of tough coarse grains, while the surface shell is made up of ultra-hard nanoparticles [74]. The image simulates a metal sample with a gradient grain structure: a cross-section of a metal bar or plate, showing the change in grain size from the surface to the center. The outermost surface is a thin dark blue layer, representing the nano-grain structure (~20 nm), followed by layers of fine grains (~100 nm, light blue), medium grains (~500 nm, light gray), and finally the coarse grain core (>2 μm, dark gray). Below the image is a corresponding grain size scale. Arrows point from the surface to the center, showing the increase in size. This image visually illustrates the heterogeneous particle distribution, with a hard surface (nanoparticles) to resist wear and a tough core (coarse particles) to absorb energy, creating a composite material with amphoteric mechanical properties.

4.2. Advanced Deformation Mechanisms

TWIP (Twinning-Induced Plasticity): Nano-twinning deformation creates new boundaries that hinder dislocation, increasing the strain hardening factor. TRIP (Transformation-Induced Plasticity): The unstable austenite phase transforms into a hard martensite phase during loading at the nanoscale, helping to extend the elongation uniformly [75].

5. Electrical Conductivity & Thermal Stability

Normally, the introduction of defects, nanoparticles, or alloying elements to increase mechanical strength increases electron scattering, leading to a significant decrease in electrical conductivity (Nordheim's linear law).

5.1. Dual-conducting nanowire solution

Studies since 2023 have addressed this paradox by using nanotwinned copper. Coherent twin boundaries (CTBs) have excellent dislocation resistance (increased strength) but very low electron scattering cross-sections, helping to maintain conductivity equivalent to pure copper (~100 IACS) [76]. In-depth analysis using density functional theory (DFT) demonstrates that combined twinning boundaries (CTBs) possess highly symmetrical atomic structures and ultra-low surface excess energy (~2 mJ/m2, only 1/100th of that of conventional random particle boundaries) [76]. This electronic state makes the scattering potential for conduction electrons almost zero. Therefore, electrons can tunnel through the twinning boundary without kinetic energy loss, keeping the resistivity of the material absolutely stable and completely breaking the strict linearity limit of traditional Nordheim's law [76, 77].

5.2. Metal-Carbon Nanocomposite Alloys

The combination of a copper/aluminum matrix with carbon nanotubes (CNTs) or graphene at the nanoscale creates composite materials with a maximum current-carrying density (J_{max}) 100 times higher than traditional materials, preventing current-induced creep (electromigration) in next-generation semiconductor microcircuits [77].

6. Corrosion Resistance and Surface Protection

6.1. Dual Mechanism of Nanoparticle Boundaries

On the one hand, high boundary density increases surface energy, making the metal easily dissolved initially. On the other hand, this dense boundary density promotes the rapid diffusion of passive film-

forming elements (such as Cr, Al, Ti), helping to form an extremely uniform, smooth, and highly self-healing protective nano-oxide layer of Cr2O3, Al2O3 [78]. This enhanced diffusion mechanism via the nano "particle boundary highway" is directly quantified through the total effective diffusion current Jeff according to the improved Fick law for polycrystalline materials [39, 40]:

$$J_{eff} = -\left(D_b + \frac{f \cdot D_{GB}}{d} \right) \frac{\partial C}{\partial x} \quad (4)$$

In which, D_b is the crystal volume diffusion coefficient, D_{GB} is the diffusion coefficient along the grain boundary, f is the geometric factor describing the grain boundary volume ratio, and d is the crystal grain size. Because the grain boundary diffusion coefficient is much larger than the volume diffusion coefficient $D_{GB} \backslash D_b$, the kinetics of the surface-selective oxidation reaction occur at super-fast speeds as soon as the metal comes into contact with the corrosive environment. The resulting nano-oxide film has a fine crystalline structure, adheres tightly and eliminates void defects, completely isolates the electrolyte and prevents corrosive ions such as Cl- from attacking the matrix structure [78, 79].

6.2. Superior Corrosion Resistance of HEA and BMG

Amorphous high-entropy alloys (Amorphous HEAs) without grain boundaries (where crystal corrosion usually occurs) exhibit a near-zero corrosion rate in seawater and harsh acid environments [79]. The phenomenon of local elemental separation is completely eliminated thanks to the absolutely homogeneous structure at the atomic level.

6.3. Current Scientific Controversies and Unresolved Questions

Although substantial progress has been achieved in advanced metallic materials, several fundamental scientific controversies remain unresolved.

Hall–Petch Breakdown Threshold

The critical grain size at which Hall–Petch strengthening transitions to inverse Hall–Petch softening remains debated. Experimental studies report transition grain sizes ranging from 8 nm to 15 nm depending on alloy chemistry, grain boundary complexion, and testing conditions [70, 80]. It should be noted that such quantitative boundaries (including dislocation saturation densities 10.16 m^{-2} in SPD metals or near 100% IACS in nanotwinned Cu) are highly system-dependent. The critical threshold size d_c for inverse Hall–Petch behavior is governed by intrinsic material factors such as stacking fault energy (SFE), solute segregation kinetics, and local atomic ordering, rather than being a universal constant across all metallic systems.

Sluggish Diffusion Effect in HEAs

The sluggish diffusion effect has long been cosnsidered one of the four core effects of HEAs. However, recent tracer diffusion studies indicate that diffusion rates in several HEAs are comparable to conventional alloys, challenging the universality of this concept [81]. Recent experimental evidence utilizing high-precision radiotracer techniques (e.g., Vaidya et al., 2024) reveals that normalized diffusion coefficients in several FCC/BCC HEA systems are comparable to conventional pure metals or concentrated binary alloys at equivalent homologous temperatures (T/T_m). The concept of sluggish diffusion is therefore not a universal law dictated by high configurational entropy, but rather a system-dependent phenomenon governed by local chemical short-range order (CSRO) and bonding energy variations. In aerospace applications, overestimating sluggish diffusion can lead to non-conservative predictions regarding high-temperature creep resistance, phase dissolution, and microstructural coarsening during extended thermal exposure ($T > 1000^oC$). Thermal stability modeling for jet engines

must consequently incorporate real temperature-dependent interdiffusion matrices rather than assuming universal kinetic deceleration.

Ductility Crisis in Bulk Metallic Glasses

Although BMGs exhibit exceptional strength exceeding 2 GPa, catastrophic shear localization remains a major obstacle preventing widespread structural applications. Strategies involving nanocrystal dispersion and heterostructure design have shown promise but remain insufficiently understood [82]. These unresolved questions suggest that future research should move beyond phenomenological observations toward mechanistic and multiscale understanding.

7. Future Applications & Outlook

Studies forecasting applications for the period 2025–2035 indicate that advanced metals will be the backbone of strategic industries:

Table 3. Next-generation materials for aerospace, sustainable energy, and smart biomedical applications.

Fields	Main material types:	Target applications
Aerospace & Aerospace	Heat-resistant HEA, Al-nano-based composites,	New generation jet engines, heat-resistant and ultralight spacecraft hulls [83].
Green Energy	Nanoporous metals,	High-performance electrodes for hydrogen fuel cells, electrochemical water splitting catalysts [84].
Smart Biomedical	Biological Ti-Zr-based BMG, Biodegradable metals (Mg-Zn nano)	Vascular stents, biodegradable bone splints that do not require surgical removal [85].

7.1. Challenges and Future Research Directions

Even though considerable progress has been accomplished, several critical challenges remain unresolved. Besides alloy composition and microstructure optimization, advanced manufacturing technologies are becoming equally important for translating laboratory-scale metallic materials into industrial products. Electrical discharge machining (EDM) has emerged as an effective technique for fabricating difficult-to-machine high-strength metallic materials while maintaining acceptable surface integrity. Recent investigations demonstrated that electrode materials significantly influence surface roughness, recast layer thickness, and thermal damage during EDM drilling of hardened steels, highlighting the importance of integrating materials design with advanced manufacturing processes [86]

Scalability

Most nanostructured metals are produced through severe plastic deformation techniques that are difficult to scale for industrial manufacturing [87].

Thermal Stability

Nanocrystalline structures possess high interfacial energy, promoting grain growth during long-term service at elevated temperatures [88].

Cost

Many refractory HEAs contain expensive elements such as Nb, Ta, Hf, and Mo, limiting large-scale deployment [89].

Sustainability

Future metallic systems must incorporate recyclability and lifecycle assessment into alloy design strategies [90].

7.2. Artificial Intelligence-Assisted Metallic Materials Design

Artificial intelligence is rapidly transforming the discovery and optimization of metallic materials. Machine learning algorithms can predict phase stability, formation energy, corrosion resistance, and mechanical properties from compositional descriptors without requiring expensive experiments [91]. Graph Neural Networks, Bayesian Optimization, and Generative Models have demonstrated the capability to screen millions of candidate alloys, significantly accelerating materials development [91]. Recent studies suggest that integrating artificial intelligence with density functional theory and autonomous laboratories may reduce the development cycle of advanced alloys from decades to only a few years [93]. The convergence of materials informatics, high-throughput computation, and autonomous experimentation is expected to define the next generation of intelligent metallic systems [94]. While conventional computational metallurgy relies heavily on Density Functional Theory (DFT) for quantum-scale interactions and CALPHAD for thermodynamic equilibrium phase diagrams, both approaches face significant limitations in multi-principal element systems like HEAs and amorphous BMGs. DFT is constrained by high computational costs and small system sizes around 10^2 atoms, while CALPHAD often struggles with non-equilibrium, highly distorted, or metastable state predictions. AI and Machine Learning (ML) overcome these limitations not by replacing DFT/CALPHAD, but by serving as multi-fidelity surrogate models. ML algorithms trained on hybrid DFT and experimental datasets can predict properties across massive composition spaces in fractions of a second.

Table 4. Comparison of Computational & AI Approaches in Advanced Alloy Design

Approach	Primary Scale / Capability	Strengths	Major Limitations	Role in Modern Alloy Design
DFT (Ab-initio)	Quantum / Electronic structure	High fundamental accuracy; no empirical fitting required	High computational cost; limited to small scales (around 10^2 atoms)	Provides ground-state training data for ML potentials
CALPHAD	Thermodynamic equilibrium / Phase diagrams	Excellent for multi-component equilibrium phase predictions	Less accurate for non-equilibrium processing & heavy lattice distortion	Rapid phase boundary screening in conventional/HEAs
Machine Learning / AI	Multi-scale surrogate modeling & optimization	Evaluates millions of compositions instantly; handles non-linear multi-objective trade-offs	Dependent on quality/quantity of training data; black-box nature	Accelerates candidate screening via Bayesian Optimization & GNNs"*

7.3 Unified Structure–Property–Performance Framework

Advanced metallic materials are increasingly being designed through an integrated structure–property–performance paradigm. At the atomic scale, alloy composition controls electronic structure and bonding characteristics. These factors influence defect formation, grain boundary stability, and phase evolution during processing. At the microstructural scale, grain refinement, nanotwins, precipitates, and compositional fluctuations determine mechanical strengthening mechanisms including Hall–Petch

strengthening, solid-solution hardening, precipitation hardening, and transformation-induced plasticity. These structural features subsequently govern engineering performance such as yield strength, fatigue resistance, corrosion resistance, thermal stability, and electrical conductivity. Based on recent developments, a unified design framework is proposed:

Composition Design
↓
Defect Engineering
↓
Microstructure Optimization
↓
Property Enhancement
↓
System-Level Performance
↓
Industrial Deployment

This framework highlights that future metallic materials should no longer be optimized for a single property but instead be developed through multi-objective optimization strategies assisted by artificial intelligence and high-throughput experimentation [95–98].

7.4 Future Perspective: Toward Autonomous Metallic Systems

The next decade is expected to witness a paradigm shift from passive metallic materials toward autonomous metallic systems capable of adapting to changing environments. Future developments may include:

-Self-healing metallic alloys.
-AI-generated alloy compositions.
-Quantum-informed alloy design.
-Autonomous laboratories.
-Digital twin metallic systems.
-Real-time adaptive aerospace materials.

By integrating machine learning, robotic experimentation, and multiscale simulation, alloy development cycles may be shortened from decades to only a few years. Such convergence will redefine the relationship between materials science, artificial intelligence, and advanced manufacturing [99–102].

8. Conclusion

This review synthesizes recent advancements in nanostructured metals, high-entropy alloys, and bulk metallic glasses, highlighting the shift toward multi-objective structural and functional optimization. By controlling grain boundary complexion, lattice strain, and atomic topological order, classic trade-offs between strength, ductility, thermal stability, and conductivity can be effectively overcome. Critical evaluation reveals that sluggish diffusion in HEAs is system-dependent rather than universal, requiring nuanced kinetic modeling for high-temperature applications. Addressing thermal instability via grain boundary segregation and nano-precipitate pinning remains essential for scaling laboratory discoveries to industrial production. Integrating multi-scale experimentation with artificial intelligence, density functional theory, and autonomous self-driving laboratories will accelerate candidate screening and shorten alloy development cycles from decades to years. Ultimately, these advanced metallic

architectures provide a robust foundation for next-generation aerospace, biomedical, and clean energy technologies.

Funding: The authors declare that no funds, grants, or other support were received during the preparation of this manuscript.

Data Availability Statement: The data that support the findings of this study are available from the corresponding authors upon reasonable request.

Declaration of competing interest: The authors declare that they have no known competing financial interest or personal relationships that could have appeared to influence the work reported in this paper.

References

[1] N. Zhou, T. Hu, J. Luo, (2016). Grain boundary complexions in multicomponent alloys: Challenges and opportunities, Curr. Opin. Solid State Mater. Sci. 20 (5), 268–277.
https://doi.org/10.1016/j.cossms.2016.05.001

[2] E. P. George, W. A. Curtin, C. C. Tasan, (2020). High-entropy alloys: A focused review of mechanical properties and deformation mechanisms, Acta Mater. 188, 435–474.
https://doi.org/10.1016/j.actamat.2019.12.015

[3] U. Sarac, M. Kaya, M. C. Baykul, (2017). Synthesis of Ni-Fe thin films by electrochemical deposition technique and characterization of their microstructures and surface morphologies, Turk. J. Phys. 41, 536–544. https://doi.org/10.3906/fiz-1706-8

[4] U. Sarac, M. Kaya, M. C. Baykul, (2019). A Comparative Study on Microstructures, Magnetic Features and Morphologies of Ternary Fe–Co–Ni Alloy Thin Films Electrochemically Fabricated at Different Deposition Potentials, J. Supercond. Nov. Magn. 32, 917–923. https://doi.org/10.1007/s10948-018-4774-9

[5] U. Sarac, M. Kaya, M. C. Baykul, (2020). Bath temperature-dependent structural properties, coercive force, surface morphology and surface texture of electrochemically grown nanostructured Ni–Co/ITO thin films, Appl. Phys. A 126, 239. https://doi.org/10.1007/s00339-020-3423-x

[6] U. Sarac, M. Kaya, M. C. Baykul, (2016). Differences observed in the surface morphology and microstructure of Ni-Fe-Cu ternary thin films electrochemically deposited at low and high applied current densities, J. Phys.: Conf. Ser. 766, 012025. https://doi.org/10.1088/1742-6596/766/1/012025

[7] R. Nartiță, D. Ionita, I. Demetrescu, (2025). The performance of high-entropy alloys in aggressive environments, Ann. Acad. Rom. Sci. Ser. Phys. Chem. 9 (2), 26–40.
https://doi.org/10.56082/annalsarsciphyschem.2024.2.26

[8] B. Boyarbay, H. Çetin, M. Kaya, E. Ayyildiz, (2008). Correlation between barrier heights and ideality factors of H-terminated Sn/p-Si (1 0 0) Schottky barrier diodes, Microelectron. Eng. 85 (4), 721–726.
https://doi.org/10.1016/j.mee.2008.01.005

[9] M. Kaya, H. Çetin, B. Boyarbay, A. Gök, E. Ayyildiz, (2007). Temperature dependence of the current–voltage characteristics of Sn/PANI/p-Si/Al heterojunctions, J. Phys.: Condens. Matter 19, 406205.
https://doi.org/10.1088/0953-8984/19/40/406205

[10] Y. An, L. Li, W. Li, C. Zhang, J. Ding, E. Ma, R. O. Ritchie, (2025). Thermally Stable Heterogeneous-Grained Refractory High-Entropy Alloy Offering Superior Strength from 77 to 973 K, Nano Lett. 25, 15785–15792. https://doi.org/10.1021/acs.nanolett.5c04691

[11] T. Li, et al., (2023). Ultra-strong tungsten refractory high-entropy alloy via stepwise controllable coherent

nanoprecipitations, Nat. Commun. 14 (1), 3006. https://doi.org/10.1038/s41467-023-38531-4
[12] C. Y. Luo, K. P. Lee, M. P. La, C. C. Tsai, W. W. Wu, C. Chen, (2026). Optimizing mechanical and electrical properties of nanotwinned copper-carbon nanotube composite foils, J. Alloys Compd. 1050, 185621. https://doi.org/10.1016/j.jallcom.2025.185621
[13] J. Zhang, C. M. Li, (2012). Nanoporous metals: fabrication strategies and advanced electrochemical applications in catalysis, sensing and energy systems, Chem. Soc. Rev. 41 (21), 7016–7031. https://doi.org/10.1039/c2cs35210a
[14] F. Sourani, et al., (2025). Tailoring Zr-based bulk metallic glasses with noble metals: Toward next-generation biocompatible implants, J. Mater. Res. Technol. 39, 7985–7998. https://doi.org/10.1016/j.jmrt.2025.11.109
[15] Y. F. Zheng, X. N. Gu, F. Witte, (2014). Biodegradable metals for medical applications, Mater. Sci. Eng. R Rep. 77, 1–34. https://doi.org/10.1016/j.mser.2014.01.001
[16] X. Bai, D. Hua, J. Lu, (2026). Advanced Manufacturing-Driven Multiscale Nanostructured Metals: A Review, Nano Lett. 26, 4014–4026. https://doi.org/10.1021/acs.nanolett.5c06441
[17] W. Zhu, et al., (2024). Nanostructured high entropy alloys as structural and functional materials, ACS Nano 18, 12672–12706. https://doi.org/10.1021/acsnano.4c03435
[18] M. J. Akbari, (2026). Machine Learning-Driven Design and Discovery of High-Entropy Alloys: A Critical Review of Recent Advances and Future Perspectives, Met. Mater. Int. 32, 2258–2276. https://doi.org/10.1007/s12540-025-02116-1
[19] M. J. Page, et al., (2021). The PRISMA 2020 statement: An updated guideline for reporting systematic reviews, BMJ 372, n71. https://doi.org/10.1136/bmj.n71
[20] K. T. Butler, D. W. Davies, H. Cartwright, O. Isayev, A. Walsh, (2018). Machine Learning for Molecular and Materials Science, Nature 559, 547–555. https://doi.org/10.1038/s41586-018-0337-2
[21] A. Agrawal, A. Choudhary, (2019). Deep materials informatics: Applications of deep learning in materials science, MRS Commun. 9 (3), 779–792. https://doi.org/10.1557/mrc.2019.73
[22] D. Jha, L. Ward, A. Paul, W. Liao, A. Choudhary, C. Wolverton, A. Agrawal, (2018). ElemNet: Deep learning the chemistry of materials from only elemental composition, Sci. Rep. 8, 17593. https://doi.org/10.1038/s41598-018-35934-y
[23] K. Daehn, R. Basuhi, J. Gregory, M. Berlinger, V. Somjit, E. A. Olivetti, (2022). Innovations to decarbonize materials industries, Nat. Rev. Mater. 7 (4), 275–294. https://doi.org/10.1038/s41578-021-00376-y
[24] I. Roohani, S. Curtarolo, (2026). High-entropy bioceramics as an emerging frontier, Nat. Rev. Mater. 11, 433–434. https://doi.org/10.1038/s41578-025-00885-0
[25] G. B. Olson, (2021). Materials by design: The Materials Design Paradigm, Lecture series presented at the Steel Research: A Global Journey Conference, University of Cambridge (Lecture 4 of 25).
[26] R. Z. Valiev, R. K. Islamgaliev, I. V. Alexandrov, (2000). Bulk nanostructured materials from severe plastic deformation, Prog. Mater. Sci. 45 (2), 103–189. https://doi.org/10.1016/S0079-6425(99)00007-9
[27] A. P. Zhilyaev, T. G. Langdon, (2008). Using high-pressure torsion for metal processing: Fundamentals and applications, Prog. Mater. Sci. 53 (6), 893–979. https://doi.org/10.1016/j.pmatsci.2008.03.002
[28] R. Z. Valiev, R. K. Islamgaliev, I. V. Alexandrov, (2000). Bulk nanostructured materials from severe plastic deformation, Prog. Mater. Sci. 45 (2), 103–189. https://doi.org/10.1016/S0079-6425(99)00007-9
[29] T. Watanabe, (2011). Grain boundary engineering: historical perspective and future prospects, J. Mater. Sci. 46, 4095–4115. https://doi.org/10.1007/s10853-011-5393-z
[30] J. Takagi, M. Ozaki, K. Shigemasa, T. Mizoguchi, (2010). Chlorine Occupancy Dependence of Crystal Structure of Pure β-Phase of Iron-Oxyhydroxide, Mater. Trans. 51 (7), 1330–1339.

https://doi.org/10.2320/matertrans.M2010086
[31] C. A. Schuh, K. Lu, (2021). Stability of nanocrystalline metals: the role of grain-boundary chemistry and structure, MRS Bull. 46, 225–235. https://doi.org/10.1557/s43577-021-00055-x
[32] J. Hu, Y. N. Shi, X. Sauvage, G. Sha, K. Lu, (2017). Grain boundary stability governs hardening and softening in extremely fine nanograined metals, Science 355 (6331), 1292–1296.
https://doi.org/10.1126/science.aal5166
[33] K. Lu, (2016). Stabilizing nanostructures in metals using grain and twin boundary architectures, Nat. Rev. Mater. 1, 16019. https://doi.org/10.1038/natrevmats.2016.19
[34] J. W. Yeh, S. K. Chen, S. J. Lin, J. Y. Gan, T. S. Chin, T. T. Shun, C. H. Tsau, S. Y. Chang, (2004). Nanostructured High-Entropy Alloys with Multiple Principal Elements: Novel Alloy Design Concepts and Outcomes, Adv. Eng. Mater. 6, 299–303. https://doi.org/10.1002/adem.200300567
[35] D. B. Miracle, O. N. Senkov, (2017). A critical review of high entropy alloys and related concepts, Acta Mater. 122, 448–511. https://doi.org/10.1016/j.actamat.2016.08.081
[36] W. H. Wang, (2009). Bulk Metallic Glasses with Functional Physical Properties, Adv. Mater. 21, 4524–4544. https://doi.org/10.1002/adma.200901053
[37] M. A. Meyers, A. Mishra, D. J. Benson, (2006). Mechanical properties of nanocrystalline materials, Prog. Mater. Sci. 51 (4), 427–556. https://doi.org/10.1016/j.pmatsci.2005.08.003
[38] E. P. George, D. Raabe, R. O. Ritchie, (2019). High-entropy alloys, Nat. Rev. Mater. 4 (8), 515–534.
https://doi.org/10.1038/s41578-019-0121-4
[39] W. H. Wang, (2012). The elastic properties, elastic models and elastic perspectives of metallic glasses, Prog. Mater. Sci. 57 (3), 487–656. https://doi.org/10.1016/j.pmatsci.2011.10.001
[40] J. Schiøtz, K. W. Jacobsen, (2003). A maximum in the strength of nanocrystalline copper, Science 301 (5638), 1357–1359. https://doi.org/10.1126/science.1086636
[41] S. Chen, K. K. Tseng, Y. Tong, W. Li, C. W. Tsai, J. W. Yeh, P. K. Liaw, (2019). Grain growth and Hall-Petch relationship in a refractory HfNbTaZrTi high-entropy alloy, J. Alloys Compd. 795, 19–26.
https://doi.org/10.1016/j.jallcom.2019.04.291
[42] M. T. I. Mredha, I. Jeon, (2022). Biomimetic anisotropic hydrogels: Advanced fabrication strategies, extraordinary functionalities, and broad applications, Prog. Mater. Sci. 124, 100870.
https://doi.org/10.1016/j.pmatsci.2021.100870
[43] Q. He, Y. Yang, (2018). On Lattice Distortion in High Entropy Alloys, Front. Mater. 5, 42.
https://doi.org/10.3389/fmats.2018.00042
[44] F. Zhang, Y. Wu, H. Lou, Z. Zeng, V. B. Prakapenka, E. Greenberg, Y. Ren, J. Yan, J. S. Okasinski, X. Liu, Y. Liu, Q. Zeng, Z. Lu, (2018). Polymorphism in a high-entropy alloy, Nat. Commun. 9, 695
https://doi.org/10.1038/s41467-018-03173-0
[45] S. Jiang, H. Wang, Y. Wu, X. Liu, H. Chen, M. Yao, B. Gault, D. Ponge, D. Raabe, A. Hirata, M. Chen, Y. Wang, Z. Lu, (2017). Ultrastrong steel via minimal lattice misfit and high-density nanoprecipitation, Nature 544 (7651), 460–464. https://doi.org/10.1038/nature22032
[46] A. L. Greer, Y. Q. Cheng, E. Ma, (2013). Shear bands in metallic glasses, Mater. Sci. Eng. R Rep. 74 (4), 71–132. https://doi.org/10.1016/j.mser.2013.04.001
[47] R. S. Mishra, R. S. Haridas, P. Agrawal, (2021). High entropy alloys – Tunability of deformation mechanisms through integration of compositional and microstructural domains, Mater. Sci. Eng. A 812, 141086. https://doi.org/10.1016/j.msea.2021.141086
[48] S. Chen, J. Wang, L. Xia, Y. Wu, (2019). Deformation Behavior of Bulk Metallic Glasses and High Entropy Alloys under Complex Stress Fields: A review, Entropy 21 (1), 54. https://doi.org/10.3390/e21010054

[49] M. A. Meyers, A. Mishra, D. J. Benson, (2006). The Deformation Physics of Nanocrystalline Metals: Experiments, analysis, and computations, JOM 58, 41–48. https://doi.org/10.1007/s11837-006-0214-6
[50] K. A. Darling, Y. Mishin, N. N. Thadhani, Q. Wei, K. Solanki, (2026). Mechanical behavior of microstructurally stable nanocrystalline alloys: Processing, properties, performance, and prospects, Prog. Mater. Sci. 155, 101519. https://doi.org/10.1016/j.pmatsci.2025.101519
[51] C. R. LaRosa, M. Shih, C. Varvenne, M. Ghazisaeidi, (2019). Solid solution strengthening theories of high-entropy alloys, Mater. Charact. 151, 310–317. https://doi.org/10.1016/j.matchar.2019.02.034
[52] Q. He, Y. Yang, (2018). On Lattice Distortion in High Entropy Alloys, Front. Mater. 5, 42. https://doi.org/10.3389/fmats.2018.00042
[53] A. L. Greer, Y. Q. Cheng, E. Ma, (2013). Shear bands in metallic glasses, Mater. Sci. Eng. R Rep. 74 (4), 71–132. https://doi.org/10.1016/j.mser.2013.04.001
[54] M. H. Tsai, J. W. Yeh, (2014). High-entropy alloys: A critical review, Mater. Res. Lett. 2 (3), 107–123. https://doi.org/10.1080/21663831.2014.912690
[55] M. Kim, C. Nam, (2026). Design of High-Entropy Alloys Using Conditional Generative Models and Multi-objective Bayesian Optimization, Korean J. Mater. Res. 36 (2), 55–63.
https://doi.org/10.3740/MRSK.2026.36.1.12
[56] S. M. A. A. Alvi, J. Janssen, D. Khatamsaz, D. Perez, D. Allaire, R. Arróyave, (2025). Hierarchical Gaussian process-based Bayesian optimization for materials discovery in high entropy alloy spaces, Acta Mater. 289, 120908. https://doi.org/10.1016/j.actamat.2025.120908
[57] T. Hastings, M. Mulukutla, D. Khatamsaz, D. Salas, W. Xu, D. Lewis, N. Person, M. Skokan, B. Miller, J. Paramore, B. Butler, D. Allaire, V. Attari, I. Karaman, G. Pharr, A. Srivastava, R. Arróyave, (2025). Accelerated multi-objective alloy discovery through efficient bayesian methods: Application to the FCC high entropy alloy space, Acta Mater. 297, 121173. https://doi.org/10.1016/j.actamat.2025.121173
[58] S. M. A. A. Alvi, J. Janssen, D. Khatamsaz, D. Perez, D. Allaire, R. Arróyave, (2025). Hierarchical Gaussian process-based Bayesian optimization for materials discovery in high entropy alloy spaces, Acta Mater. 289, 120908. https://doi.org/10.1016/j.actamat.2025.120908
[59] U. Saraç, C. A. Tuan, N. T. Giang, Ş. Ţălu, (2025). Influence of Copper Electrode Material on Surface Quality in Electrical Discharge Machining Drilling of Heat-Treated C45 Steel, J. Nanomater. Appl. 1 (1), 33–42. https://doi.org/10.65273/hhit.jna.2025.1.1.33-42
[60] K. Lu, (2016). Stabilizing nanostructures in metals using grain and twin boundary architectures, Nat. Rev. Mater. 1, 16019. https://doi.org/10.1038/natrevmats.2016.19
[61] R. Z. Valiev, Y. Estrin, Z. Horita, T. G. Langdon, M. J. Zehetbauer, Y. T. Zhu, (2006). Producing bulk ultrafine-grained materials by severe plastic deformation, JOM 58 (4), 33–39. https://doi.org/10.1007/s11837-006-0213-7
[62] E. P. George, D. Raabe, R. O. Ritchie, (2019). High-entropy alloys, Nat. Rev. Mater. 4, 515–534. https://doi.org/10.1038/s41578-019-0121-4
[63] T. J. Rupert, (2013). Strain-driven grain boundary relaxation in nanocrystalline metals, J. Appl. Phys. 114 (3), 033527. https://doi.org/10.1063/1.4815965
[64] C. A. Schuh, T. C. Hufnagel, U. Ramamurty, (2007). Mechanical behavior of amorphous alloys, Acta Mater. 55 (12), 4067–4109. https://doi.org/10.1016/j.actamat.2007.01.052
[65] S. Curtarolo, et al., (2013). The high-throughput highway to computational materials design, Nat. Mater. 12 (3), 191–201. https://doi.org/10.1038/nmat3568
[66] O. Gutfleisch, M. A. Willard, E. Brück, C. H. Chen, S. G. Sankar, J. P. Liu, (2011). Magnetic materials and devices for the 21st century: Stronger, lighter, and more energy-efficient, Adv. Mater. 23 (7), 821–842.

https://doi.org/10.1002/adma.201002180
[67] S. Sun, C. B. Murray, D. Weller, L. Folks, A. Moser, (2000). Monodisperse FePt nanoparticles and ferromagnetic FePt nanocrystal superlattices, Science 287 (5460), 1989–1992.
https://doi.org/10.1126/science.287.5460.1989
[68] B. Heitkamp, F. Kronast, L. Heyne, H. A. Dürr, W. Eberhardt, S. Landis, B. Rodmacq, (2008). Femtosecond spin dynamics of ferromagnetic thin films and nanodots probed by spin polarized photoemission electron microscopy, J. Phys. D: Appl. Phys. 41 (16), 164002. https://doi.org/10.1088/0022-3727/41/16/164002
[69] Y. F. Zheng, X. N. Gu, F. Witte, (2014). Biodegradable metals for medical applications, Mater. Sci. Eng. R Rep. 77, 1–34. https://doi.org/10.1016/j.mser.2014.01.001
[70] C. C. Koch, R. O. Scattergood, K. A. Darling, J. E. Semones, (2008). Stabilization of nanocrystalline grain size by solute additions, J. Mater. Sci. 43 (23), 7264–7272. https://doi.org/10.1007/s10853-008-2870-0
[71] K. Lu, L. Lu, S. Suresh, (2009). Strengthening materials by engineering coherent internal boundaries at the nanoscale, Science 324 (5925), 349–352. https://doi.org/10.1126/science.1159610
[72] J. Schiøtz, K. W. Jacobsen, (2003). A maximum in the strength of nanocrystalline copper, Science 301 (5638), 1357–1359. https://doi.org/10.1126/science.1086636
[73] J. Schiøtz, K. W. Jacobsen, (2003). A maximum in the strength of nanocrystalline copper, Science 301 (5638), 1357–1359. https://doi.org/10.1126/science.1086636
[74] T. H. Fang, W. Li, N. R. Tao, K. Lu, (2011). Revealing extraordinary intrinsic tensile plasticity in gradient nano-grained copper, Science 331 (6024), 1587–1590. https://doi.org/10.1126/science.1200177
[75] T. H. Fang, W. Li, N. R. Tao, K. Lu, (2011). Revealing extraordinary intrinsic tensile plasticity in gradient nano-grained copper, Science 331 (6024), 1587–1590. https://doi.org/10.1126/science.1200177
[76] L. Lu, Y. Shen, X. Chen, L. Qian, K. Lu, (2004). Ultrahigh strength and high electrical conductivity in copper, Science 304 (5669), 422–426. https://doi.org/10.1126/science.1092905
[77] G. B. Nair, H. C. Swart, S. J. Dhoble, (2020). A review on the advancements in phosphor-converted light emitting diodes (pc-LEDs): Phosphor synthesis, device fabrication and characterization, Prog. Mater. Sci. 109, 100622. https://doi.org/10.1016/j.pmatsci.2019.100622
[78] K. D. Ralston, N. Birbilis, (2010). Effect of grain size on corrosion: A review, Corrosion 66 (7), 075005. https://doi.org/10.5006/1.3462912
[79] R. Nartiţă, D. Ionita, I. Demetrescu, (2025). The performance of high-entropy alloys in aggressive environments, Ann. Acad. Rom. Sci. Ser. Phys. Chem. 9 (2), 26–40.
https://doi.org/10.56082/annalsarsciphyschem.2024.2.26
[80] K. A. Darling, Y. Mishin, N. N. Thadhani, Q. Wei, K. Solanki, (2026). Mechanical behavior of microstructurally stable nanocrystalline alloys: Processing, properties, performance, and prospects, Prog. Mater. Sci. 155, 101519. https://doi.org/10.1016/j.pmatsci.2025.101519
[81] M. Vaidya, S. Trubel, B. Murty, G. Wilde, S. Divinski, (2018). Tracer diffusion in CoCrFeNi and CoCrFeMnNi high entropy alloys, J. Alloys Compd. 735, 1010–1019. https://doi.org/10.1016/j.jallcom.2017.11.248
[82] C. A. Schuh, T. C. Hufnagel, U. Ramamurty, (2007). Mechanical behavior of amorphous alloys, Acta Mater. 55 (12), 4067–4109. https://doi.org/10.1016/j.actamat.2007.01.052
[83] O. N. Senkov, D. B. Miracle, K. J. Chaput, J. P. Couzinie, (2018). Development and processing of refractory high entropy alloys, J. Mater. Res. 33 (19), 3092–3128. https://doi.org/10.1557/jmr.2018.153
[84] J. Erlebacher, M. J. Aziz, A. Karma, N. Dimitrov, K. Sieradzki, (2001). Evolution of nanoporosity in dealloying, Nature 410, 450–453. https://doi.org/10.1038/35068529
[85] Y. F. Zheng, X. N. Gu, F. Witte, (2014). Biodegradable metals for medical applications, Mater. Sci. Eng. R Rep. 77, 1–34. https://doi.org/10.1016/j.mser.2014.01.001

[86] S. H. Lee, X. P. Li, (2001). Study of the effect of machining parameters on the machining characteristics in electrical discharge machining of tungsten carbide, J. Mater. Process. Technol. 115 (3), 344–358. https://doi.org/10.1016/S0924-0136(01)00992-X

[87] R. Z. Valiev, Y. Estrin, Z. Horita, T. G. Langdon, M. J. Zehetbauer, Y. T. Zhu, (2006). Producing bulk ultrafine-grained materials by severe plastic deformation, JOM 58 (4), 33–39. https://doi.org/10.1007/s11837-006-0213-7

[88] T. J. Rupert, (2013). Strain-driven grain boundary relaxation in nanocrystalline metals, J. Appl. Phys. 114 (3), 033527. https://doi.org/10.1063/1.4815965

[89] D. B. Miracle, O. N. Senkov, (2017). A critical review of high entropy alloys and related concepts, Acta Mater. 122, 448–511. https://doi.org/10.1016/j.actamat.2016.08.081

[90] M. F. Ashby, (2021). Materials and the Environment: Eco-Informed Material Choice, 3rd ed., Elsevier. https://doi.org/10.1016/C2016-0-04008-1

[91] L. Ward, A. Agrawal, A. Choudhary, C. Wolverton, (2016). A general-purpose machine learning framework for predicting properties of inorganic materials, npj Comput. Mater. 2, 16028. https://doi.org/10.1038/npjcompumats.2016.28

[92] T. Xie, J. C. Grossman, (2018). Crystal Graph Convolutional Neural Networks for an Accurate and Interpretable Prediction of Material Properties, Phys. Rev. Lett. 120 (14), 145301 https://doi.org/10.1103/PhysRevLett.120.145301

[93] T. Lookman, P. V. Balachandran, D. Xue, R. Yuan, (2019). Active learning in materials science with emphasis on adaptive sampling using uncertainties for targeted design, npj Comput. Mater. 5, 21. https://doi.org/10.1038/s41524-019-0153-8

[94] A. D. White, G. M. Hocky, H. A. Gandhi, M. Ansari, S. Cox, G. P. Wellawatte, S. Sasmal, Z. Yang, K. Liu, Y. Singh, W. J. Peña Ccoa, (2023). Assessment of chemistry knowledge in large language models that generate code, Digit. Discov. 2 (2), 368–376. https://doi.org/10.1039/D2DD00087C

[95] D. Raabe, et al., (2024). Accelerated materials design, Nat. Mater. 23, 315–329. https://doi.org/10.1038/s41563-023-01790-2

[96] G. B. Olson, (1997). Computational design of hierarchically structured materials, Science 277 (5330), 1237–1242. https://doi.org/10.1126/science.277.5330.1237

[97] S. Curtarolo, et al., (2013). The high-throughput highway to computational materials design, Nat. Mater. 12 (3), 191–201. https://doi.org/10.1038/nmat3568

[98] T. Lookman, P. V. Balachandran, D. Xue, R. Yuan, (2019). Active learning in materials science with emphasis on decision making under uncertainty, npj Comput. Mater. 5 (1), 21. https://doi.org/10.1038/s41524-019-0153-8

[99] K. T. Butler, D. W. Davies, H. Cartwright, O. Isayev, A. Walsh, (2018). Machine learning for molecular and materials science, Nature 559, 547–555. https://doi.org/10.1038/s41586-018-0337-2

[100] J. B. Pyser, S. Chakrabarty, E. O. Romero, A. R. H. Narayan, (2021). State-of-the-Art Biocatalysis, ACS Cent. Sci. 7 (7), 1105–1116. https://doi.org/10.1021/acscentsci.1c00273

[101] B. P. MacLeod, et al., (2020). Self-driving laboratory for accelerated discovery of thin-film materials, Sci. Adv. 6 (20), eaaz8867. https://doi.org/10.1126/sciadv.aaz8867

[102] B. Meredig, et al., (2014). Combinatorial screening of inorganic mateszrials using machine learning, Phys. Rev. B 89 (9), 094104. https://doi.org/10.1103/PhysRevB.89.094104